WATER RESOURCES RESEARCH, VOL. 30, NO. 4, PAGES 857–864, APRIL 1994

Colloid transport in unsaturated porous media

Jiamin Wan[1] and John L. Wilson

Department of Geoscience, New Mexico Institute of Mining and Technology, Socorro

Abstract. This paper explores the significance of the gas-water interface on colloid sorption and transport. Three types of common saturation conditions were simulated in packed sand columns: (1) a completely water-saturated condition, (2) gas bubbles trapped by capillary forces as a nonwetting residual phase (15% gas), and (3) gas present as a continuous phase (46% gas), or in other words, a vadose zone situation. Different saturations provided different interfacial conditions. Two types of polystyrene latex particles (0.2 μm), hydrophilic and hydrophobic, were used in each of the three saturations. Relative surface hydrophobicity of latex particles was characterized by contact angle measurements. Each experiment was repeated five times. A total of 30 columns with good reproducible packing and gas content gave reproducible particle breakthrough curves. The retention of both hydrophilic and hydrophobic colloids increased with gas content of the porous medium. Colloids preferentially sorbed onto the gas-water interface relative to the matrix surface. The degree of sorption increased with the increase of colloid surface hydrophobicity. The results validate and quantify direct microscopic scale visualization observations made in two-dimensional pore network glass micromodels (Wan and Wilson, 1994). These findings suggest an additional mechanism for filtration and for particulate transport in the subsurface environment, whenever more than one fluid phase is present. The results also give clear evidence that the presence of inadvertently trapped residual gas could help explain the discrepancy between water-saturated laboratory column experiments and related theory.

Introduction

The transport of mobile colloids through porous media is an important process in both natural and engineering systems. In subsurface hydrogeological environments, colloid transport significantly facilitates the migration of colloidal and colloid-bound pollutants in groundwater and soils [*McDowell-Boyer et al.*, 1986; *Gschwend and Wu*, 1985; *Buddemeier and Hunt*, 1988; *McCarthy and Zachara*, 1989; *Bales et al.*, 1991; *Puls and Powell*, 1992]. In the water and wastewater treatment industries, granular bed filtration separates fine particles, pathogens and colloid-associated pollutants from suspensions [e.g., *Ives and Gregory*, 1966; *Yao et al.*, 1971; *O'Melia*, 1989]. Historically, research on colloid transport has focused on water-saturated porous media. Quantitative models for predicting particle transport are presented in the water filtration literature [*Yao et al.*, 1971; *Spielman and FitzPatrick*, 1973; *FitzPatrick and Spielman*, 1973; *Tien and Payatakes*, 1979; *Tien*, 1989]. These models account for the deposition mechanisms of particle-medium collisions and the conditions for particle deposition. For Brownian particles, diffusion and advection control the collision rate. Deposition is determined by the interfacial forces between the mobile particles and fixed solid surfaces (collectors). These forces include electrostatic, van der Waals, hydration, and hydrodynamic forces. A particle immersed in a solvent often perturbs the local ordering of the "structure" of the solvent molecules. If the free energy associated with this perturbation varies with the distance between the two approaching particles, it produces an additional "solvation" or "structure" force between them. When water is the solvent, it is called the hydration force [*Israelachvili*, 1992]. The deposition rate in an ideal medium can be calculated theoretically from the solution of the convective diffusion equation [*Spielman and Friedlander*, 1974; *Friedlander*, 1977; *Adamczyk et al.*, 1983]. The deposition rate can also be determined experimentally by measuring the particle capture rate through a clean granular bed [e.g., *Gregory and Wishart*, 1980; *Tobiason and O'Melia*, 1988]. A large discrepancy between controlled laboratory experiments and theory is a common feature of colloid transport studies. For instance, when interfacial forces are repulsive the predictions of transport distance greatly exceed any laboratory or field observations [*Bowen and Epstein*, 1979; *Elimelech and O'Melia*, 1990a, b]. Various reasons for these discrepancies have been proposed over the past two decades [e.g., *Gregory and Wishart*, 1980; *Adamczyk et al.*, 1983; *O'Melia*, 1989; *Elimelech and O'Melia*, 1990a; *Litton and Olson*, 1993]. Among these are heterogeneous surface roughness, differences in surface charge and surface potential, and differences in the methods of collector surface preparation, etc. However, none of these previous investigators has mentioned the effect of a residual gas phase present in porous media. This paper provides evidence for the preferential deposition of colloids onto the gas-water interface that significantly reduces the transport distance. Some of the discrepancies in standard single-phase flow experiments can be explained by the inadvertent presence of trapped residual gas.

[1]Now at Lawrence Berkeley Laboratory, Berkeley, California.

Paper number 93WR03017.
0043-1397/94/93WR-03017$05.00

Table 1. Latex Particles and Their Surface Properties

Used in	Particle Type	Size, μm	Contact Angle θ_a	Zeta Potential,* mV
Column experiment	carboxylate hydrophilic latex	0.19	36 ± 6°	−53
Column experiment	sulfate hydrophobic latex	0.22	127 ± 5°	−36
Micromodel experiment†	fluorescent carboxylate hydrophilic latex	0.95	<10°	−89
Micromodel experiment†	fluorescent sulfate hydrophobic latex	1.05	122 ± 7°	−48

*Electrophoretic mobilities were measured in the solution of 1.0 m*M* $NaNO_3$ and *p*H 6.6 at 24°C.

†From *Wan and Wilson* [1994].

Contaminant transport through unsaturated porous media is an important aspect of subsurface transport phenomena. Colloids generated from weathering, biological activities, and human influence may be much more concentrated in soil water compared to their levels in groundwater. How these colloids move through the vadose zone and capillary fringe to reach the water table is not well understood. In particular, the role of the gas-water interface, one of the most important interfaces in the vadose zone, has been neglected. In two-dimensional glass micromodels, *Wan and Wilson* [1992b, 1994] used microscopy to study the interactions between various colloids (latex spheres, bacteria, and clay particles) and the solid-water and gas-water interfaces on a microscopic pore scale. They visually observed the preferential sorption of particles onto the gas-water interface, which they explain by, among other things, a capillary force acting on particles at the gas-water interface. We chose general terms "sorption/desorption" in this paper to describe the results of surface interactions, which do not refer to any underlying mechanism. The terms "capture," "deposition," or even "attachment" could be used instead, but the more general term "sorption" appears appropriate for a gas-water interface which can move, particularly since the particles can themselves move along this interface. We will reexamine two of *Wan and Wilson*'s [1994] experiments, which used latex particles similar to those employed in this paper. Because they were interested in visualization, their particles were larger (1.0 μm) and fluorescent. As recalled in Table 1, they used a relatively hydrophilic carboxylate latex and a relatively hydrophobic sulfate latex. Suspensions of the particles were injected into clean etched glass micromodels, composed of a two-dimensional quadrilateral network of three-dimensional pores. The models contained residual air bubbles, trapped in the pore bodies, as shown in Figures 1 and 2. Pore bodies and throats were sized at about 200 μm and 50 μm in diameter, respectively. The entire model was about 2.5 cm long and 2.0 cm wide, with a pore volume of about 0.2 mL, in 1200 pore bodies connected by pore throats. The chemistry conditions, ionic strength (1.0 m*M* $NaNO_3$) and *p*H (6.6), were the same as in the column experiments presented below. Figures 1 and 2 are photomicrographs taken after a slug of 30 pore volumes of dilute particle suspensions was injected and then replaced by a slug of three pore volumes of particle-free solution. In Figure 1, hydrophilic latex particles (contact angle <10°, 0.95 μm) are preferentially sorbed onto a gas bubble trapped in a pore body, with few particles sorbed onto the adjacent pore walls. *Wan and Wilson* [1994] hypothesized that the hydration force between the gas-water interface and the particle may be attractive; also the flow hydrodynamics may give some

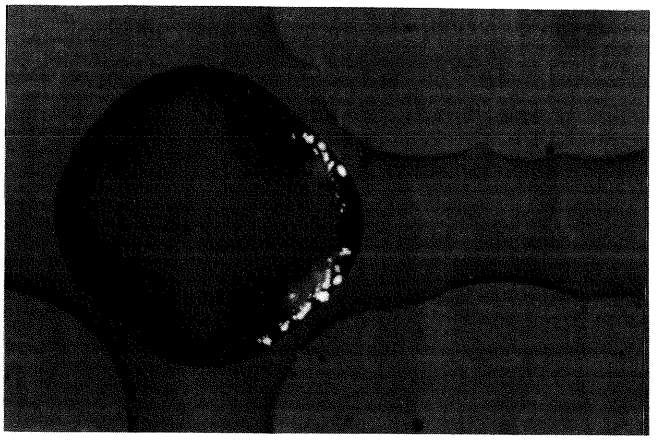

Figure 1. Hydrophilic negatively charged latex particles (0.95 μm) preferentially sorb onto the downstream portion of an air bubble. Few particles sorb onto the pore walls. Solution ionic strength is 1.0 m*M*, *p*H 6.6. Glass micromodel with quadrilateral network. (Not previously published.)

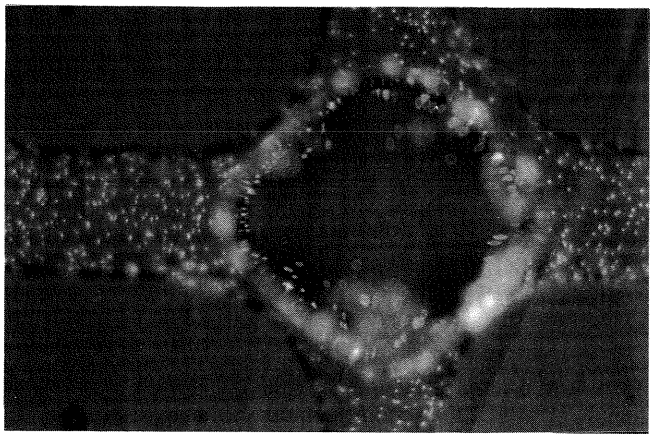

Figure 2. Hydrophobic negatively charged latex particles sorb onto both air-water and glass-water interfaces. Observe the effect of particle surface hydrophobicity by comparing to Figure 1. All the other experimental conditions are the same. (From *Wan and Wilson* [1994].)

particles enough momentum to penetrate the energy barrier and then capillary forces rupture and hold the particles on the interface. In Figure 2, hydrophobic latex particles (contact angle equal to 122°, 1.05 μm) are sorbed onto both the pore walls and the trapped bubble. Relatively hydrophobic particles show a stronger affinity for the gas-water interface than the hydrophilic particles. Both hydration and capillary forces increase with particle hydrophobicity.

The objective of this paper is to validate and quantify those visualized phenomena on a hydrologically significant scale within a typical porous medium, sand, with similar surface and aqueous chemistry. Column experiments are described in which colloid suspensions are injected at one end and breakthroughs observed at the other end. Water and gas saturations are varied from experiment to experiment in order to observe the effect of the gas-water interface on breakthrough. Fully water-saturated experiments serve as the control. Other experiments are performed with capillary-trapped residual gas bubbles (15% gas saturation), and with a continuous gas phase (46% gas saturation). In the residual gas experiments the gas-water interface is isolated on individual bubbles, as in *Wan and Wilson*'s [1994] visualization experiments. Here we test their hypothesis that some particles will be retained, due to irreversible sorption on the isolated bubbles. The continuous gas phase experiments contain a continuous and largely interconnected gas-water interface. Solving the Navier-Stokes equations for two-phase gas-water flow in a single water-wet pore, modeled as a circular tube, leads to the conclusion that water velocity will be maximum along the gas-water interface [*Bird et al.*, 1960]. In the continuous gas phase experiments we test the hypothesis that colloids sorbed at this continuous interface will move faster than the average water velocity and will break through early. However, packed bed porous media are geometrically far more complex than a single-tube model [*Bear*, 1972], and it is quite possible that particles attached to the gas-water interface will become trapped. The continuous gas phase experiments also have a much larger interfacial area between gas and water, suggesting much greater sorption than for the isolated bubbles. We also tested transport for two different types of colloid particles with different surface properties in order to further elucidate processes at the gas-water interface. Finally, in order to avoid being misled by experimental errors, we repeated each column experiment five times. The experimental procedure was finalized when reproducible results were obtained.

Materials and Methods

General Methodology

Particle hydrophobicity and column gas saturation were the only two variables in the column experiments. Two types of 0.2-μm-diameter polystyrene latex particles (relatively hydrophilic and hydrophobic) were used; each type was tested for three different gas saturations. Each experiment was repeated five times, for a total of 30 column experiments. Figure 3 schematically illustrates the three different saturations. In Figure 3a, the columns were fully water saturated; the quartz-water interface was the only interface present. These experiments acted as a control for the unsaturated flow experiments. In Figure 3b, the columns contained a capillary trapped residual gas phase occupying 15% of the pore space; two interfaces were present: the gas-water and quartz-water. The pore scale geometry for water flow was altered by the gas bubbles trapped in the pore bodies. In Figure 3c, the columns were also unsaturated, but the gas occupied 46% of the pore space as a continuous phase. Both gas and water were interconnected, as was the interface between them. Water saturation geometry changed significantly. Experiments were performed in 30-cm-long and 2.5-cm-ID borosilicate glass chromatography columns (ACE Glass, Inc.) packed with 212- to 315-μm-diameter quartz sand (Unimin Company). The cleaning procedure for the sand is described below. The columns were mounted vertically and flow was directed downward by peristaltic pumps (WIZ pumps, ISCO). The pumping rate was adjusted for each column individually to maintain a constant seepage velocity at 10.0 cm/h, as described later. Ionic strength was 1.0 mM ($NaNO_3$), and pH was 6.6 buffered by $NaNO_3$ for all of the solution and suspensions. The particle number concentration of the influent suspension was approximately 5×10^{10} L^{-1}. Relative particle concentrations were measured with a double-beam spectrophotometer (Perkin Elmer 330) at a wavelength of 260 nm. Prior to colloid addition, solutions were filtered with a 0.22-μm pore size filter. Particle suspensions, made with the filtered solution, were also filtered (2.5 μm, Whatman 5) to remove any particle aggregates. Air was used as the gas phase.

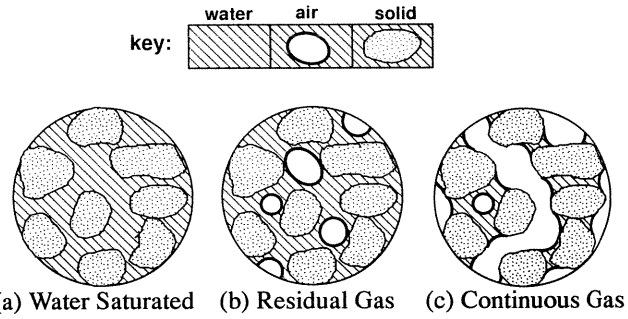

Figure 3. Three types of columns representing three types of groundwater conditions: (a) fully water-saturated; (b) residual gas bubbles; (c) continuous gas and water phases.

Some abbreviations have been used in the following text: D water denotes distilled water; 2D water denotes distilled and deionized water; 3D water denotes distilled, deionized, and degassed water (3D water was made by boiling 2D water and storing it in a container connected to a vacuum system); 2D solution denotes solution made by using 2D water; 3D solution denotes solution made by using 3D water. In the experiments, 3D water and 3D solution were used in the water saturated columns to maintain an air-free condition; 2D water and 2D solution were used in unsaturated columns to keep the gas from dissolving.

Colloids and Surface Characterization

Four types of surfactant-free polystyrene latex microspheres (Interfacial Dynamics Corporation), their surface zeta potentials, and water contact angles are listed in Table 1. The first two latexes listed were used in these column experiments. The remaining two latexes, used by *Wan and Wilson* [1994], are bigger, but have similar surface chemistry. Particle electrophoretic mobility was measured with a Coulter DELSA 440 (Doppler electrophoretic light scattering analyzer) in a solution of 1.0 mM $NaNO_3$ and pH 6.6 at

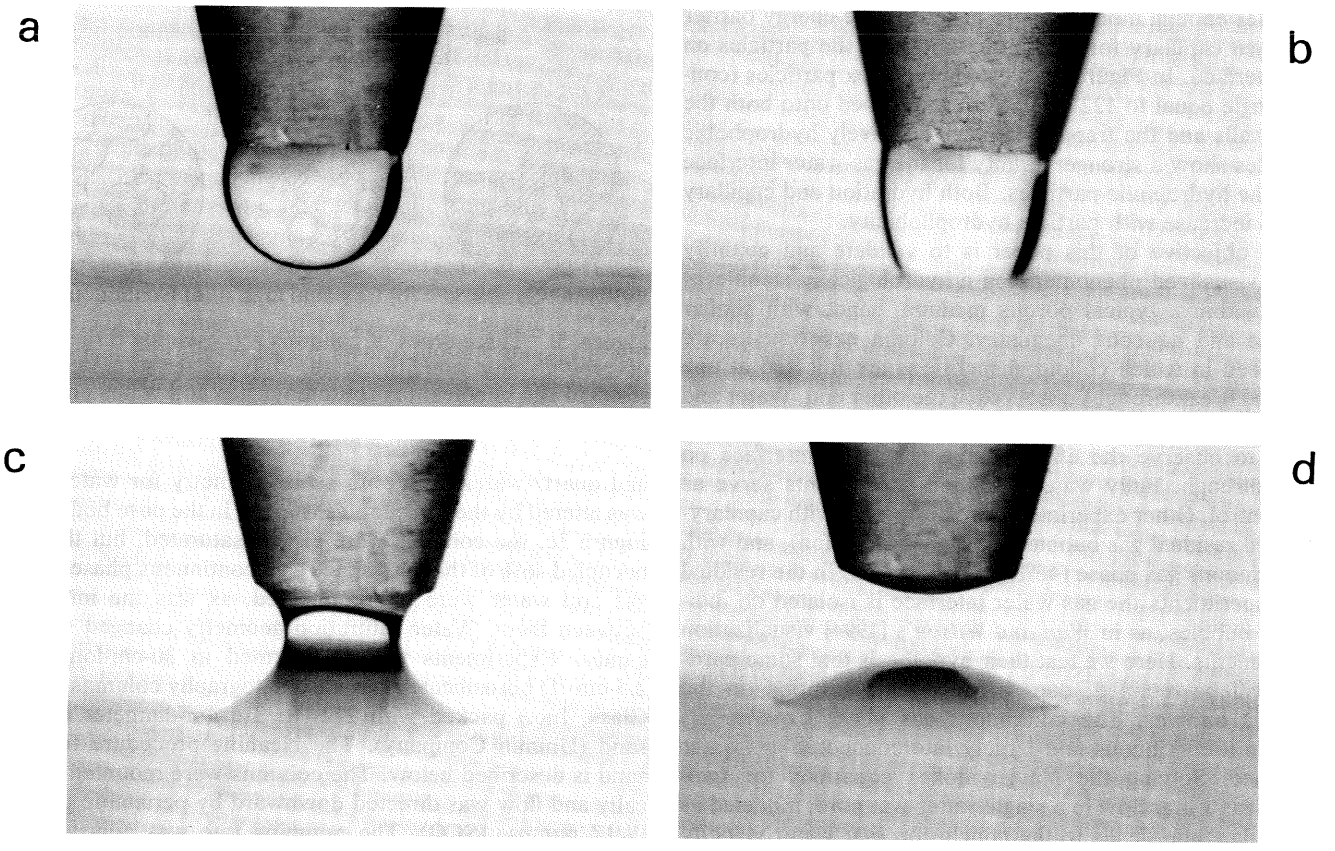

Figure 4. Contact angle measurement with particle layer–captive drop method used on hydrophobic latex particles: (a) before the water drop attaches to the particle layer; (b) as the advancing contact angle is measured; (c) as the receding contact angle is measured; (d) when measurement is finished.

25°C. The accuracy and precision of the Coulter instrument operation were assessed through analysis of a hydrophilic electrophoresis standard particle, as determined by the manufacturer (Interfacial Dynamics Corporation). Mobility data were converted to zeta potentials calculated from the measured mean electrophoretic mobility by using the tabulated numerical calculations of *Ottewill and Shaw* [1972].

Particle hydrophobicity is an important factor controlling particle stability in an aqueous phase, but unfortunately, a quantitative measurement is not yet available. A conventional way to roughly estimate surface hydrophobicity/hydrophilicity is to use electrophoretic mobility, zeta potential, or surface charge density. The last two parameters can be calculated from measured electrophoretic mobility with certain assumptions. All three of these parameters are, in general, a measurement of surface charge state. The relation among the three is complex and poorly understood [*Elimelech and O'Melia*, 1990c]. The general relationship is that the smaller the absolute number of the zeta potential, the lower the charge density, or the lower the electrophoretic mobility, the more hydrophobic the particle surface, and vice versa. This type of estimate is not accurate enough for our purpose. Contact angle is a better measurement for latex surface hydrophobicity than electrophoretic mobility. We measured contact angles of smear layers of latex particles with a classic captive drop method [*Gaudin et al.*, 1963]. A few drops of particle sludge (highly concentrated particle suspension) were put on a clean glass slide, and a flat sludge layer was made by simply shaking the slide. The slide was then allowed to dry in a desiccator until the particle layer began to crack (it took about 3 hours). The thickness of the layer was about 50–100 μm. The contact angle at the junction of the layer, air, and liquid drop (a solution of 10^{-3} M $NaNO_3$, pH 6.6) was measured. The readings were taken 2 s after the liquid drop attached to the layer. Each contact angle listed in Table 1 was the mean of 15 measurements. Figure 4 shows a measurement of a contact angle on the hydrophobic particles used in the column experiments. A glass slide with a smeared particle layer was set under the pipet in all four pictures. Figure 4a was taken just before the water drop attached to the surface. The shape of the water drop was not symmetric, which was the result of an imperfection in the pipet tip. Figure 4b was taken after the water drop attached to the surface while all three phases were equilibrating with each other. The advancing contact angle was then measured. The contact angles were not constant but relaxed because of a slow process of imbibition into the packed particle layer. Afterward the water drop was pulled slowly off of the surface. Figure 4c records the moment just before the water drop slapped off the tip of the pipet when the receding contact angle was measured. We did not report the receding contact angle because of the large hysteresis of the system. Figure 4d is a picture taken after the measurement was finished. The accuracy of this smear layer–captive drop method is limited by many factors, including the roughness of the particle layer and pipet tip, particle size,

and moisture content of the layer. The measured values are relative, not absolute, indicators of hydrophobicity.

Preparation of Medium Surface

A clean medium surface is one of the most important factors controlling the reproducibility of particle deposition rate (from our own experience as well as that of *Litton and Olson* [1993]). The quartz sand was size-fractionated with stainless steel sieves to a 212–315 μm range. In order to reduce surface contaminants and remove attached amorphous and fine material, we used an elaborate cleaning procedure. About 500 g of sorted dry sand was placed in a 1000-mL glass beaker and soaked in 50% HNO_3 solution for 24 hours. The sand was then boiled in a fresh 50% HNO_3 for 20 min, followed by a batch wash with D water 20–30 times until the pH reached that of the D water. Afterward the sand was soaked in a 1.0% sodium polyphosphate solution and sonicated for 20 min. (Polyphosphates "sequester" calcium ion in a soluble or suspended form, thus detaching fine clay particles from sand surfaces.) In the next step the sand was batch washed with D water until the pH reached that of the D water. The sand was sonicated in 2D water for 20 min, then batch washed with 2D water five times. Finally, the sand was dried in a clean oven at 110°C for 24 hours.

Preparation of the Columns

A column apparatus consisted of a glass chromatographic column, 30 cm long and 2.5 cm ID with two tetrafluoroethylene (TFE) end caps and associated plumbing. The end caps were screwed into threaded ends on the glass column and sealed against the column with O rings. A network of small channels, approximately 1 mm deep and 1.5 mm wide, was machined onto the surface of each end cap. The grooves allow for a more uniform water flow between the end caps and the sand pack. A polypropylene filter with a mesh opening of 105 μm was glued onto each end cap in order to keep fine sand particles from leaving the column. The effective column volume was accurately measured gravimetrically for each individual packing.

The columns were prepared by following this procedure: Gas was removed from a measured amount of cleaned and dried sand by sonicating it in 3D water for 20 min. The sand was washed three times with 3D water to remove any fine particles. Using a vibrator the column was wet packed with special care to avoid any layering. Sand left from packing was dried and weighed to determine the net amount of sand used. Any remaining air trapped during packing was dissolved by flooding 3D water through the packed column until completely water-saturated, as judged gravimetrically. The porosity of the column was then calculated by using measured column volume, the weight of sand used, the density of the sand, and the final weight of the fully saturated column. For an unsaturated experiment the column was thoroughly drained. For an unsaturated column with residual gas bubbles a 2D solution was then imbibed into the medium at a low flow rate (~6 cm/h) in order to entrap air as a residual phase of gas bubbles. The column was weighed and the gas and water saturation calculated. For an unsaturated column with a continuous gas phase a 2D solution was pumped into the column from the top at a rate which appeared to result in a seepage velocity of 10 cm/h. We define the seepage velocity v as $v = Q/AS_w n$, where Q is the volumetric pumping rate, n is the porosity, A is column cross-section area, and S_w is the water saturation. We measured n and S_w and adjusted Q to obtain a constant seepage velocity, v. Starting with a small constant flow rate, we increased the pumping rate and water saturation monotonically until the seepage velocity reached 10 cm/h. Table 2 lists the parameters and their reproducibility. For example, porosity was 0.43 ± 0.02 over the total of 30 columns. The gas saturation S_g ($S_w + S_g = 1$) of the 10 unsaturated columns with a residual gas phase was $S_g = 15.0 \pm 0.6\%$, and for the remaining 10 unsaturated columns with a continuous gas phase it was $S_g = 46.0 \pm 2.4\%$. The pH was controlled at 6.68 ± 0.12 over all of the experiments by adding $NaHCO_3$. These strictly controlled physical and chemical parameters ensured the reproducibility of the column experiments.

Table 2. Parameters of Column Experiments

Parameters	Value
Size of sand grains	212–315 μm
Bulk density	1.65 ± 0.01 g/cm^3
Porosity	0.43 ± 0.02
Residual gas saturation	15.0 ± 0.6%
Continuous gas saturation	46.0 ± 2.4%
Seepage velocity	10.0 cm/hr
Ionic strength	1.0 mM
pH	6.68 ± 0.12
Column weight changes	−0.10 ± 0.05%

Experimental Procedure

Each column was flooded with a 3D solution until the pH and turbidity of the effluent reached that of the influent. The pumping rate (milliliters per hour) was adjusted to match the seepage velocity of 10.0 cm/h. A slug of dilute particle suspension (5×10^{10}/L) was then injected at the seepage velocity of 10.0 cm/h. The slug was one water pore volume for hydrophilic particles and six pore volumes for hydrophobic particles. For a total column pore volume V, a water pore volume was calculated as $S_w V$. The effluent was collected by a fraction collector at a rate of six samples per pore volume. Two or three pore volumes of particle-free solution were injected to replace the suspension at the same flow rate. The particle-free solution had the same ionic strength and pH as the suspensions. At the end of the run the column weight and effluent pH value were checked. Relative particle concentrations of influent C_0 and effluent C were measured with the spectrophotometer. Most of the 30 experiments included a bromide tracer in the slug of suspension. The bromide showed a sharp breakthrough with no evidence for preferential flow or tailing. Examples of these breakthrough curves, for early test columns, are given by *Wan and Wilson* [1992a].

Results and Discussion

Hydrophilic Colloids

A slug of one water pore volume of hydrophilic latex particle (0.19 μm, $\theta_a = 36°$) suspension was applied in the three types of differently saturated columns and then displaced by two pore volumes of particle-free solution. All of the other experimental conditions were kept strictly the same for all of the columns. Therefore the differences in the

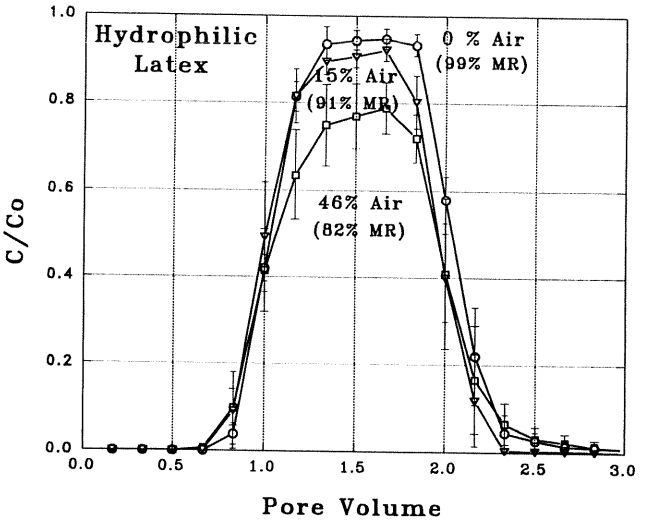

Figure 5. Breakthrough curves of hydrophilic latex particles from three types of columns: fully saturated, unsaturated with gas bubbles, and unsaturated with a continuous gas phase. Each curve shows an average of five repeated experiments, and the standard deviations are plotted as error bars. Percentages show the percentage of pore volume occupied by air (% Air) as well as the percentage of total mass recovery (% MR).

breakthrough data were mainly caused by the presence and amount of gas. The results are presented as breakthrough curves where the fraction of the influent particle concentration (C/C_0) leaving the packed column is a function of pore volume. C and C_0, respectively, were the effluent and influent concentrations of colloids. The percentage of total mass recovery for each breakthrough curve is the integration of the mass concentrations from all of the effluent fractions normalized by the total mass of the influent. Because of our interest in transport processes in the subsurface we use mass recovery, rather than mass retained, as in the filtration literature. The influent particle concentration C_0 was analyzed at the same time as the effluent C, and the volume of influent suspension was closely controlled.

Figure 5 is the summary of results from 15 columns with hydrophilic particles. The top curve is the breakthrough curve from the water-saturated columns, the middle curve is from the columns with a trapped residual gas phase, and the lower curve is from the unsaturated columns with a continuous gas phase. The solid lines were drawn with the average of the data from five repeated experiments. The standard deviation of each point is plotted as a vertical error bar. These curves present several features. First, the standard deviations of the breakthrough curves are small, relative to the great difficulties in reproducing data in filtration experiments, indicating good reproducibility. Second, the mass recoveries decrease systematically with increasing gas saturation. The total mass recovery for each saturation was 99% from the water-saturated columns, 91% from the residual gas columns, and 82% from the continuous gas columns. The 99% mass recovery from the water-saturated medium was caused by the chemical conditions, which were unfavorable for particle attachment to solid surfaces. This curve also indicates that mechanical filtration, including caking and straining, did not have a significant effect on particle transport through the packed medium and that, therefore, all the particles retained in the columns were retained due to physical-chemical filtration. Increasing the air saturation to 15.0% of pore volume lowered the mass recovery by 8%. Where did this mass go? *Wan and Wilson*'s [1994] micromodel experiment, shown in Figure 1, suggests the answer: The 8% mass was sorbed onto the air bubbles trapped in the pore bodies. Increasing the air saturation further to the continuous air phase condition decreased the mass recovery by 17% compared to the water saturated condition. We believe that this was caused partly by the increased area of the gas-water interface, creating more sorption sites and higher collision probabilities. It is possible that the presence of thin water films and wedges, around air-filled pores, may also have caused some straining. However, *Wan and Wilson*'s [1994] observations in the micromodels suggest that most of the retained particles were sorbed onto the gas-water interface. Third, the seepage velocity was maintained the same for the columns with different water saturations. Breakthrough of $C/C_0 = 0.5$ occurs at about the same time in all 30 columns. No preferential movement was observed, even for the columns with the continuous gas phase. We reject the hypothesis, raised earlier, that sorption onto the gas-water interface leads to faster particle movement and early breakthrough. It appears that in these continuous gas phase columns, particles sorbed locally along the gas-water interface and were unable to move very far. Fourth, there is some increase of breakthrough curve dispersion with gas saturation as observed in Figure 5. The moderate nature of the increase may be due to the uniformly sized sand grains and the decreased significance of flow tortuosity induced by trapped gas in a uniform pore structure for the residual gas columns. The increase is larger for the continuous gas columns. Fifth, the curves from the unsaturated columns have no significant tailing, consistent with irreversible sorption onto the gas-water interface.

These experiments confirm *Wan and Wilson*'s [1994] visual observation. Hydrophilic particles are sorbed irreversibly onto the gas-water interface under typical groundwater conditions. Many types of the natural inorganic colloids, such as clay and other mineral fines, are in this hydrophilic category. The sorption mechanisms are not very well understood yet, but it is clear that there is an attractive force between the gas-water interface and the particle which is not related to the quartz surface.

Hydrophobic Colloids

The behavior of hydrophobic latex particles (0.22 μm, $\theta_a = 127°$) was tested and compared with that of the hydrophilic ones. A slug of six water pore volumes of particle suspension was fed into the columns and then displaced by three water pore volumes of particle-free solution. The larger slug of suspension was applied because of the strong retention of hydrophobic particles. For a slug of one water pore volume suspension, no particles broke through from the unsaturated columns. All of the other experimental conditions were kept strictly the same. Using visual evidence like the micromodel photomicrograph in Figure 4, *Wan and Wilson* [1994] found that few particles entered into areas of thin water films where the gas bubbles contact the solid surface. This observation suggests that the total effective sorption area of the solid medium is reduced with increasing gas saturation. When we interpreted the

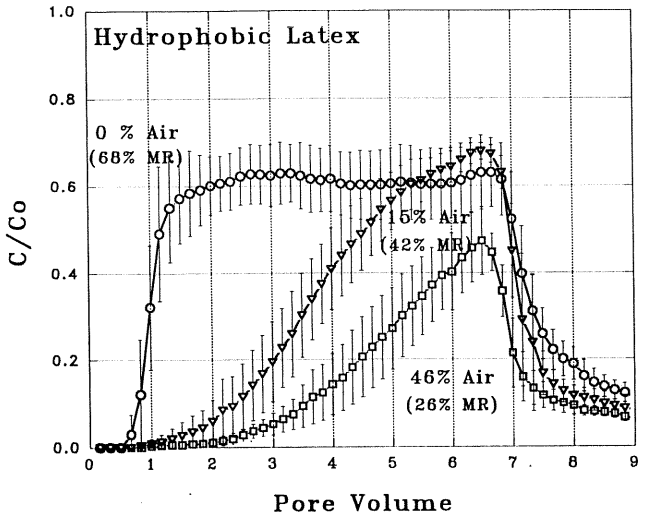

Figure 6. Breakthrough curves of hydrophobic latex particles from three types of columns: fully saturated, unsaturated with gas bubbles, and unsaturated with a continuous gas phase. Each curve shows an average of five repeated experiments, and the standard deviations are plotted as error bars. Compare the effect of particle hydrophobicity on retention with Figure 5.

mass recovery data for different saturations, we neglected this difference and assumed that the amounts of particles sorbed on the solid-water interface were the same in the different saturation conditions. There were, therefore, more particles retained by sorption on the gas-water interface than we interpreted below.

Figure 6 summarizes the results, where the breakthrough curves are from the three types of columns under different levels of saturation. Again, every experiment was repeated five times, and the breakthrough curves were drawn based on the average values. The actual mass recoveries were greater than those values shown in Figure 6 because effluent particle concentration had not yet diminished to zero when the tests were terminated. Interpretation of the curves yields several observations. First, the top curve from water-saturated columns has 68% of mass recovery, and 32% of the particles were retained in the columns. Looking at the glass micromodel pore walls in Figure 2 indicates that the retained particles sorbed onto the solid matrix surface. The plateau of the curve in Figure 6 implies that the sorption sites of the solid medium have not yet been saturated by particles, and the sorption capacity of the solid surface has not yet been reduced by the increased coverage. The obvious tailing shows desorption of particles from the solid surface. In Figure 1, hydrophilic particles do not sorb onto the pore walls, and in Figure 5 we obtained 99% mass recovery from the saturated porous medium. The net surface interaction potential at the solid surface changed from repulsive to attractive for hydrophobic particles. This was caused by a reduction of the electrostatic repulsive force between the particles and the solid surface; hence the van der Waals attractive force became dominant. Second, the middle curve from columns with trapped residual gas bubbles recovered 42% and left 58% of the particles in the column by sorption onto both solid and gas bubble surfaces, very similar to the micromodel result shown in Figure 2. Assuming that the same amount, 32%, was retained by sorption on the solid-water interface as shown by the breakthrough curve from water-saturated columns, at least 26% of the particles were retained by sorption onto the bubbles. Sorption onto the gas bubbles is believed due to hydrophobic forces between two hydrophobic surfaces: air bubble and particle surfaces. The breakthrough curve is smooth and has a gentle slope, which suggests that the sorption capacity of the gas-water interface decreases with surface coverage. The lower tailing from the unsaturated columns compared with that from saturated columns suggests that desorption is mainly from the solid-water interface. It indicates that the attractive potential between particle and bubble is greater than that between particle and matrix. This irreversibility is caused by the capillary force [*Wan and Wilson*, 1994], perhaps with a contribution from the attractive hydrophobic force. Third, the bottom curve for the continuous gas columns is similar to the middle one for the trapped gas. The only difference is that the total gas-water interface area is larger and retains more particles. A total of 74% of the particles were retained in the unsaturated columns with a continuous 46% gas saturation. Assuming that 32% of the total mass sorbed onto the water-solid interface as the top curve shows, at least 42% of the total mass sorbed onto the gas bubbles.

We also tested latex particles with a higher hydrophobicity (0.22 μm, θ_a = 140°), and observed much lower mass recoveries. For example, a slug of six pore volume particle suspension never broke through from the columns with 46% trapped gas. Because of the poor data reproducibility (caused by formation of aggregates) we will not further report the results here.

Comparing the data in Figure 6 with those in Figure 5, we see that the degree of sorption onto the gas-water interface increases with increasing particle surface hydrophobicity. In subsurface environments, organic colloids are relatively hydrophobic, and the surface hydrophobicity of inorganic colloids will increase with a sorbed covering of organic matter.

Conclusions

1. Gas saturation is a factor controlling colloid transport in the subsurface environment. As confirmed in these experiments, colloid particles preferentially sorb onto the gas-water interface relative to the solid matrix surface under typical groundwater conditions. The amount of sorption onto both the gas-water interface and the solid matrix surface dramatically increased with increasing colloid surface hydrophobicity. Hydrophobic particles have a strong affinity to the gas-water interface, but even hydrophilic particles sorb. The column results are consistent with irreversible sorption onto the gas-water interface caused by a capillary force attraction. The preferential and irreversible sorption of colloidal particles onto the gas-water interface suggests a significant transport mechanism. A stationary gas phase behaves as a sorbent phase retaining the particles, thereby reducing colloid transport. However, moving interfaces occurring during drainage, imbibition, or a bubbling process may increase the movement of colloids, perhaps down to the deeper vadose zone and underlying aquifer.

2. The effects of a capillary-trapped nonwetting gas phase in laboratory and field colloid filtration experiments have not previously attracted attention. The porous media,

thought to be water saturated, may actually be unsaturated and contain gas bubbles trapped as a residual phase. It has been demonstrated in this research that for relatively hydrophobic particles, even a small amount of residual gas can dramatically affect the transport. This issue has been essentially overlooked in published filtration experiments.

3. Although the column method has been commonly used in laboratory research, it has been demonstrated in this research that under accurately controlled physical and chemical conditions, a greater degree of reproducibility has been achieved than in previous research.

4. The direct contact angle measurement, such as described in this paper, is a better way to characterize the surface hydrophobicity of latex particles than electrophoretic mobility.

Acknowledgments. We would like to express our deep appreciation to Jill Buckley, Norman Morrow, and Robert Bowman for their helpful discussions and the use of their equipment. We would also like to acknowledge the Subsurface Science Program, Office of Health and Environmental Research, U.S. Department of Energy for supporting this work (DOE grant DE-FG03-92ER61484).

References

Adamczyk, Z., T. Dabros, J. Czarnecki, and T. G. M. van de Ven, Particle transfer to solid surfaces, *Adv. Colloid Interface Sci.*, *19*, 183–252, 1983.

Bales, R. C., S. R. Hinkle, T. W. Kroeger, and K. Stocking, Bacteriophage adsorption during transport through porous media: Chemical perturbations and reversibility, *Environ. Sci. Technol.*, *25*, 2088–2095, 1991.

Bear, J., *Dynamics of Fluids in Porous Media*, Elsevier, New York, 1972.

Bird, R. B., W. E. Steward, and E. N. Lightfoot, *Transport Phenomena*, John Wiley, New York, 1960.

Bowen, B. D., and N. Epstein, Fine particle deposition in smooth parallel-plate channels, *J. Colloid Interface Sci.*, *72*, 81–97, 1979.

Buddemeier, R. W., and J. R. Hunt, Transport of colloidal contaminants in groundwater: Radionuclide migration at the Nevada Test Site, *Appl. Geochem.*, *3*, 535–548, 1988.

Elimelech, M., and C. R. O'Melia, Effect of particle size on collision efficiency in the deposition of Brownian particles with electrostatic energy barriers, *Langmuir*, *6*, 1153–1163, 1990a.

Elimelech, M., and C. R. O'Melia, Kinetics of deposition of colloidal particles in porous media, *Environ. Sci. Technol.*, *24*, 1528–1536, 1990b.

Elimelech, M., and C. R. O'Melia, Effect of electrolyte type on the electrophoretic mobility of polystyrene latex colloids, *Colloids Surf.*, *44*, 1528–1536, 1990c.

FitzPatrick, J. A., and L. A. Spielman, Filtration of aqueous latex suspensions through beds of glass spheres, *J. Colloid Interface Sci.*, *43*, 350–360, 1973.

Friedlander, S. K., *Smoke, Dust, and Haze: Fundamentals of Aerosol Behavior*, 317 pp., Wiley-Interscience, New York, 1977.

Gaudin, A. M., A. F. Witt, and T. G. Decker, Contact angle hysteresis: Principles and application of measurement methods, *Trans. Soc. Min. Eng. AIME*, *226*, 107–112, 1963.

Gregory, J., and A. J. Wishart, Deposition of latex particles on alumina fibers, *Colloids Surf.*, *1*, 313–334, 1980.

Gschwend, P. M., and S. C. Wu, On the constancy of sediment-water partition coefficients of hydrophobic organic pollutants, *Environ. Sci. Technol.*, *19*, 90–96, 1985.

Israelachvili, J. N., *Intermolecular and Surface Force*, Academic, San Diego, Calif., 1992.

Ives, K. J., and J. Gregory, Surface forces in filtration, *Proc. Soc. Water Treat. Exam.*, *15*, 93–115, 1966.

Litton, G. M., and T. M. Olson, Colloid deposition rates on silica bed media and artifacts related to collector surface preparation methods, *Environ. Sci. Technol.*, *27*, 185–193, 1993.

McCarthy, J. F., and J. M. Zachara, Subsurface transport of contaminants, *Environ. Sci. Technol.*, *23*, 496–502, 1989.

McDowell-Boyer, L. M., J. R. Hunt, and N. Sitar, Particle transport through porous media, *Water Resour. Res.*, *22*, 1901–1921, 1986.

O'Melia, C. R., Particle-particle interactions in aquatic systems, *Colloids Surf.*, *39*, 255–271, 1989.

Ottewill, R. H., and J. N. Shaw, Electrophoretic studies of polystyrene lattices, *J. Electroanal. Chem. Interfacial Electrochem.*, *37*, 133–142, 1972.

Puls, R. W., and R. M. Powell, Transport of inorganic colloids through natural aquifer material: Implications for contaminant transport, *Environ. Sci. Technol.*, *26*, 614–621, 1992.

Spielman, L. A., and J. A. FitzPatrick, Theory for particle collection under London and gravity forces, *J. Colloid Interface Sci.*, *42*, 607–623, 1973.

Spielman, L. A., and S. K. Friedlander, Role of electrical double-layer in particle deposition by convective diffusion, *J. Colloid Interface Sci.*, *46*, 22–31, 1974.

Tien, C., *Granular Filtration of Aerosols and Hydrosols*, Butterworth, Stoneham, Mass., 1989.

Tien, C., and A. C. Payatakes, Advances in deep bed filtration, *AIChE J.*, *25*, 737–759, 1979.

Tobiason, J. E., and C. R. O'Melia, Physicochemical aspects of particle removal in depth filtration, *J. Am. Water Works Assoc.*, *80*, 54–64, 1988.

Wan, J., and J. L. Wilson, Colloid transport and the gas-water interface in porous media, in *Colloid and Interfacial Aspects of Groundwater and Soil Cleanup*, edited by D. Sabatini and R. Knox, pp. 55–70, American Chemical Society, Washington, D. C., 1992a.

Wan, J., and J. L. Wilson, New findings on particle transport within the vadose zone: The role of the gas-water interface, in *Proceedings, 12th Annual Hydrology Days*, edited by H. J. Morel-Seytoux, pp. 402–419, Hydrology Days Publications, Atherton, Calif., 1992b.

Wan, J., and J. L. Wilson, Visualization of the role of the gas-water interface on the fate and transport of colloids in porous media, *Water Resour. Res.*, *30*, 11–23, 1994.

Yao, K. M., M. T. Habibian, and C. R. O'Melia, Water and wastewater filtration: Concepts and applications, *Environ. Sci. Technol.*, *5*, 1105–1112, 1971.

J. Wan, Lawrence Berkeley Laboratory, Mail Stop 50E, 1 Cyclotron Road, Berkeley, CA 94720.

J. L. Wilson, Department of Geoscience, New Mexico Institute of Mining and Technology, Socorro, NM 87801.

(Received March 5, 1993; revised September 23, 1993; accepted October 15, 1993.)